



Cite this: *Sustainable Food Technol.*, 2026, 4, 1126

## Extrusion-driven metabolic shifts in composite flour from coffee and plantain byproducts

Laura Sofía Torres-Valenzuela,<sup>a</sup> Carolina Franco-Urbano,<sup>a</sup> Diana Paola Navia-Porras,<sup>b</sup> Jose Luis Plaza-Dorado<sup>a</sup> and Mónica P. Cala<sup>c</sup>

This study outlines the effects of extrusion on the metabolomic profile and functional properties of composite flour produced from coffee pulp, plantain rachis, and rejected plantain. Metabolomic analysis using liquid chromatography–mass spectrometry and gas chromatography–mass spectrometry revealed that 124 metabolites showing differential abundance between nonextruded flours (NEF) and extruded flours (EF). Of these, 83% (103 metabolites) decreased and 17% increased after extrusion. Global trends revealed decreases in carbohydrates, glycerophospholipids, organic acids, flavonoids, and quinic acid derivatives, whereas amino acids and alkaloids displayed mixed responses. In terms of phenolic compounds, extrusion reduced the contents of several compounds, such as procyanidins, catechins, and chlorogenic acids, but markedly increased the content of quercetin. These changes represent an increase in total phenolic content (from  $5.38 \pm 0.60$  to  $7.92 \pm 1.00$  mg GAE g<sup>-1</sup>, dry basis) and antioxidant activity (from  $50.82 \pm 3.44\%$  to  $72.62 \pm 5.87\%$ ). A slight reduction in crude protein was observed; however, protein bioavailability significantly improved with thermomechanical processing. Overall, extrusion modified the metabolomic profile of the composite flour and improved its functional and nutritional attributes, highlighting the relevance of this technology for producing precooked flour from byproducts as a promising ingredient for the production of value-added and sustainable foods.

Received 17th October 2025  
Accepted 2nd December 2025

DOI: 10.1039/d5fb00698h

rsc.li/susfoodtech

### Sustainability spotlight

This work advances sustainable food production by valorizing coffee and plantain byproducts into nutritionally enhanced precooked flours through extrusion technology. By transforming agro-industrial residues into functional food ingredients, the study contributes to circular bioeconomy principles and promotes waste reduction, resource efficiency, and value recovery within the food supply chain. The process demonstrated measurable improvements in bioactive compound content, antioxidant activity, and protein bioavailability, highlighting its potential for sustainable formulation of food products. This research directly aligns with the United Nations Sustainable Development Goals (SDGs) 2—Zero Hunger, 9—Industry, Innovation and Infrastructure, and 12—Responsible Consumption and Production, supporting the transition toward more resilient and resource-efficient food systems.

## 1. Introduction

The development of food alternatives from agro-industrial plant residues for both human and animal consumption is essential for advancing sustainability and reducing waste. Residues such as husks, seeds, stalks, bagasse, and pulp contain valuable nutrients, including proteins, fibers, fatty acids, vitamins, minerals, and antioxidant compounds.<sup>1</sup> These components can be transformed into functional foods, supplements, or food ingredients. Many phytochemicals present in postharvest residues of fruits and vegetables offer health benefits and are

applied in the management of cardiovascular diseases, diabetes, and several cancers.<sup>2</sup> The utilization of fruit and vegetable residues reduces food loss, minimizes the environmental impact of waste disposal, and contributes to food security by diversifying nutrient sources, optimizing resource use, and promoting circular economic practices. According to the FAO, approximately 1.3 billion tons of food are wasted or lost annually worldwide, 50% of which originates from fruits and vegetables, primarily during the processing and postharvest stages.<sup>3</sup>

In Colombia, coffee and plantain production chains hold significant potential for residue valorization because of their broad cultivation across various regions. Both crops are closely linked to rural areas and primary production systems.<sup>4</sup> Coffee is among the most widely traded agricultural commodities and one of the most consumed beverages worldwide, generating substantial volumes of processing residues. Approximately 0.9 kilograms of waste are produced for every kilogram of coffee fruit processed.<sup>5</sup> Among these, coffee pulp alone accounts for 40

<sup>a</sup>Grupo de Investigación GIPAB, Escuela de Ingeniería de Alimentos, Universidad del Valle, Calle 13 No. 100-00, Building E32, 760032, Cali, Colombia. E-mail: laura.torres@correounivalle.edu.co

<sup>b</sup>Grupo de Investigación Biotecnología, Facultad de Ingeniería, Universidad de San Buenaventura Cali, 76001, Cali, Colombia

<sup>c</sup>MetCore – Metabolomics Core Facility, Universidad de los Andes, Bogotá, Colombia



to 50 percent of the total fruit mass and is notably rich in phenolic compounds, dietary fiber, and other bioactive constituents.<sup>6</sup> Coffee pulp is a residue generated after the wet milling of the harvested bean, while rachis and rejected plantain are residues obtained from the postharvest of plantain. The nutritional and physicochemical qualities of flour mixtures of these residues were determined according to previously described methods.<sup>7</sup> The mixtures were subjected to thermo-mechanical extrusion treatment to improve the availability of their nutrients and bioactive compounds.

Extrusion is a versatile, fast, and scalable operation that is widely used in human and animal food production.<sup>8</sup> Reports indicate that thermomechanical treatments such as extrusion reduce antinutritional compounds, including caffeine, which may be undesirable in animal diets.<sup>9</sup> Extrusion has also been shown to improve protein digestibility, dietary fiber levels, and the bioavailability of bioactive compounds.<sup>10,11</sup> Evaluating the effects of extrusion on the metabolites of coffee and plantain byproduct blends is necessary to confirm nutritional benefits and explore applications in food formulations for both human and animal use.

Metabolomic profiling has emerged as a powerful analytical strategy in food science for comprehensively characterizing the small-molecule composition of raw materials and processed products. By capturing global metabolite shifts, this approach enables the identification of processing-induced biochemical transformations, including degradation, synthesis, or release of bioactive compounds. As a result, metabolomics provides deeper insights into how different processing techniques—such as extrusion—affect the nutritional, functional, and sensory properties of food matrices.<sup>12</sup> Metabolomic profiling of plant materials provides essential insights into key metabolites that define potential applications. Advanced techniques such as LC-MS/MS and GC-MS are widely used to identify bioactive molecules, including phenolics, flavonoids, amino acids, and volatile organic compounds,<sup>13,14</sup> and can detect processing-induced shifts in these compounds.<sup>12</sup> No previous metabolomics study has examined a blend of coffee pulp flour, rejected plantain, and plantain rachis. This work represents a novel investigation of how extrusion affects the combined metabolite profile of these residues. Therefore, this study aimed to evaluate the effect of thermomechanical extrusion on the metabolomic profile of composite flours produced from coffee and plantain byproducts, contributing to the sustainable valorization of agro-industrial residues through their potential use as nutritious food ingredients.

## 2. Materials and methods

### 2.1 Raw materials, chemical reagents, and equipment

Agro-industrial byproducts—coffee pulp (CP), plantain rachis (PR), and rejected plantain (RP)—were collected in Trujillo, Colombia (4°12'41" N, 76°19'13" W; 1317 masl). CP, PR and RP were processed using a cutting machine (Poli, Cali, Colombia), an ED 115 forced convection oven (Binder, Germany), an M20 laboratory mill (IKA, Germany), and a Ro-Tap sieve (W. S. TYLER, USA), respectively. Extrusion was conducted using

a DS32-II twin-screw extruder (Jainin Saixin Machinery Co<sup>®</sup>, Jinan, China).

For the antioxidant activity assays, DPPH and ABTS<sup>•+</sup> reagents were prepared. The 2,2 diphenyl-1-picrylhydrazyl (DPPH) (Merck, Germany) reagent was prepared by dissolving 1 mg of DPPH in methanol to obtain an absorbance of 1.00 at 490 nm. The ABTS<sup>•+</sup> radical was obtained by mixing 3.6 mg mL of 2,2'-azino-bis(3-ethylbenzothiazoline-6-sulfonic acid) (ABTS) (Merck, Germany) 14 mM and 0.662 mL of potassium persulfate (0.45 mM) (Merck, Germany). The mixture was kept in the dark for 16 h at room temperature and then diluted with methanol to an absorbance of 0.7 at 630 nm.<sup>15</sup> Trolox reagent ((±)-6-hydroxy-2,5,7,8-tetramethyl-chroman-2-carboxylic acid) (Sigma-Aldrich, USA) was used for the TEAC assay. Stock solutions of gallic acid (0–500 mg L<sup>-1</sup>) were prepared in water for the total phenolic content assay.

### 2.2 Flour processing and extrusion process

Composite flour and extruded flour were prepared according to a previously described methodology.<sup>7</sup> Briefly, PR and RP were cut, and all the byproducts (PR, RP, and CP) were dried at 45 °C to 10 ± 1% moisture. After milling and sieving (<0.425 mm), the flours were blended in proportions of 36.4% CF, 33.3% RP, and 30.3% PR. This proportion was selected according to a previously optimized formulation previously reported,<sup>7</sup> designed to provide a balanced nutritional composition and appropriate properties for extrusion.

The mixture was divided into nonextruded flour (NEF, control) and extruded flour (EF). The EF was adjusted to 18% moisture (wet basis) before extrusion. A twin-screw extruder with three thermal zones (100, 160, and 120 °C) and a 5-mm nozzle was used. The power supply frequencies were 18 Hz (input) and 36 Hz (output). The extrudates (11.5% moisture) were cooled at 25 °C for 4 h, milled, and sieved (40 mesh). EF and NEF were stored in sealed polypropylene bags at 25 °C for analysis. All experiments were carried out in quintuplicate using independent batches for each treatment ( $n = 5$ ).

### 2.3 Protein and fat composition

Protein and fat contents were determined following AOAC protocols. Protein was measured using the Kjeldahl method, using a coefficient of 6.75.<sup>16</sup> The fat content was determined using the Soxhlet extraction method.<sup>17</sup> The results are expressed as g/100 g of sample.

### 2.4 Determination of bioavailable protein

Bioavailable protein was determined in NEF and EF. The assay followed the K-PDCAAS 12/19 method.<sup>18</sup> Briefly, 0.5 g of each sample was suspended in 19 mL of 0.06 N HCl solution, vortexed for 10 s and incubated at 37 °C and 300 rpm for 30 minutes. The gastric digestion phase was simulated by adding pepsin solution (1 mL, 1 mg mL<sup>-1</sup>), after which the samples were vortexed and incubated under the same conditions. Intestinal digestion was simulated by adjusting the pH to 7.4 with 2 mL of 1.0 M Tris buffer, followed by the addition of 200 µL of trypsin/chymotrypsin solution (5 mg mL<sup>-1</sup>). The samples



were incubated for 4 h at 37 °C with continuous agitation (300 rpm). The digestion was stopped by boiling the samples in a thermostatic bath for 10 min, vortexing, and cooling to room temperature for 20 min. The undigested proteins were precipitated with 5.55 mL of trichloroacetic acid (40%), vortexed for 30 s, incubated at 4 °C for 16 h, and centrifuged at 15 000 rpm for 10 min. The supernatant was collected, and the protein content was determined by the Kjeldahl method, as described in Section 2.3.

## 2.5 Antioxidant activity and total phenolic content

**2.5.1 Extraction procedure.** Extractions were carried out by mixing 100 mg of sample with a methanol : water solution (50 : 50, v/v). The mixture was sonicated in an ultrasonic bath (TI-H-15, Elma®, USA) at 60 °C for 60 min and centrifuged (BX: C882, Unico®, USA) at 10 000 rpm for 10 min. The antioxidant activity of the supernatant was measured by DPPH, ABTS, and total phenolic content (TPC) assays. Predilution was performed as follows: 1 : 20 v/v (extract: 30% v/v ethanol solution) for DPPH and ABTS and 1 : 4 v/v for TPC.

**2.5.2 Antioxidant assays.** The antioxidant activity and total phenolic content of NEF and EF were determined through DPPH and TEAC. For the DPPH assay, 20 µL of diluted extract (1 : 20 v/v) was mixed with 180 µL of DPPH solution. The absorbance was measured at 490 nm at 90-second intervals for 30 min in a microplate reader (800TSUV-Biotech, BMG Labtech®, Germany). DPPH scavenging activity was calculated and expressed as a percentage.<sup>15</sup> For the TEAC assay, 20 µL of Trolox standard (0 to 70 µM diluted in methanol) or diluted extract was mixed with 180 µL of ABTS<sup>•+</sup> solution.<sup>19</sup> The absorbance of the mixture was measured at 630 nm at 90-second intervals for 90 min. The percentage inhibition was expressed as TEAC. The total phenolic content (TPC) was determined using the Folin-Ciocalteu method.<sup>15</sup> For this purpose, 20 µL of diluted extract (1 : 4 v/v) was mixed with 75 µL of sodium carbonate (10%) and 100 µL of Folin-Ciocalteu reagent (1 : 9, v/v diluted in distilled water). The mixture was incubated in the dark for 2 h, and the absorbance was read at 630 nm. The results are expressed as gallic acid equivalents (GAE g<sup>-1</sup> dry mass) using a calibration curve.

## 2.6 Untargeted metabolomics analysis

**2.6.1 Sample preparation for LC-QTOF-MS and GC-QTOF-MS analysis.** For LC-QTOF-MS analysis, 30 mg of sample (EF or NEF) was extracted with 500 µL of methanol (MeOH, -20 °C). The mixture was vortexed for 10 minutes, sonicated for 10 minutes, and vortexed again for 5 min. The resulting extracts were filtered through 0.22 µm membrane filters prior to analysis. Additionally, for GC-QTOF-MS analysis, 70 µL of the LC-MS extracts were dried in a SpeedVac concentrator at 35 °C for 1 h. Then, 10 µL of O-methoxyamine hydrochloride in pyridine (15 mg mL<sup>-1</sup>) was added, and the mixture was vortexed at 3200 rpm for 5 min and incubated in the dark at room temperature for 16 h. Derivatization was completed by adding 10 µL of N,O-bis(trimethylsilyl)trifluoroacetamide (BSTFA) containing 1% trimethylchlorosilane (TMCS), followed by

vortexing for 5 min and incubation at 70 °C for 1 h. After cooling to room temperature for 30 min, 50 µL of methyl stearate in heptane (5 mg L<sup>-1</sup>) was added as an internal standard. The mixture was then vortexed again at 3200 rpm for 5 minutes before analysis.

**2.6.2 Sample analysis by LC-QTOF-MS.** The samples were analyzed using an Agilent Technologies 1290 Infinity II Liquid Chromatography system coupled to a Q-TOF 6545 quadrupole time-of-flight mass spectrometer equipped with an electrospray ionization (ESI) source. A volume of 2 µL of each extract was injected into a C18 column (InfinityLab Poroshell 120 EC-C18, 100 × 2.1 mm, 1.9 µm) maintained at 40 °C. Chromatographic separation was performed using gradient elution with mobile phase A consisting of 0.1% (v/v) formic acid in Milli-Q water and mobile phase B consisting of 0.1% (v/v) formic acid in acetonitrile at a constant flow rate of 0.4 mL min<sup>-1</sup>. Mass accuracy was ensured throughout the analysis by continuous infusion of two reference masses, *m/z* 121.0509 (C<sub>5</sub>H<sub>4</sub>N<sub>4</sub>) and *m/z* 922.0098 (C<sub>18</sub>H<sub>8</sub>O<sub>6</sub>N<sub>3</sub>P<sub>3</sub>F<sub>24</sub>), in positive ion mode and *m/z* 112.9856 [C<sub>2</sub>O<sub>2</sub>F<sub>3</sub>(NH<sub>4</sub>)] and *m/z* 1033.9881 (C<sub>18</sub>H<sub>18</sub>O<sub>6</sub>N<sub>3</sub>P<sub>3</sub>F<sub>24</sub>) in negative ion mode. Detection was carried out in full scan mode (100–1100 *m/z*).

**2.6.3 Sample analysis by GC-QTOF-MS.** Data acquisition was performed using an Agilent Technologies 7890 B gas chromatograph coupled to an Agilent Technologies GC/Q-TOF 7250 time-of-flight mass selective detector equipped with a split/splitless injection port (250 °C, split ratio 50 : 1) and an Agilent Technologies 7693 A autosampler. The electron ionization (EI) source was operated at 70 eV. An Agilent Technologies J&W HP-5MS column (30 m × 0.25 mm × 0.25 µm) was used with helium as the carrier gas at a constant flow rate of 0.7 mL min<sup>-1</sup>. The oven temperature was programmed from 60 °C (1 min), ramped at 10 °C min<sup>-1</sup> to 325 °C, and held for 10 min. The transfer line, ion source filament, and quadrupole temperatures were maintained at 280 °C, 230 °C, and 150 °C, respectively. Mass spectrometry detection was performed in the range of 50–600 *m/z* at a scan rate of 5 spectra per s.

**2.6.4 Data processing, normalization, and statistical analysis.** The raw data obtained from the LC-QTOF-MS system were processed using Agilent MassHunter Profinder (version B.10.0) for feature deconvolution, alignment, and integration. For the GC-QTOF-MS data, chromatographic peak deconvolution, alignment, and integration were performed using Agilent Unknowns Analysis (version B.10.0), MassProfiler Professional (version 15.0), and Agilent MassHunter Quantitative Analysis (version B.10.00), respectively. After data extraction, all the datasets were normalized using systematic error removal using the random forest (SERRF) algorithm (<https://slfan2013.github.io/SERRF-online/>). After normalization, the data from all the analytical platforms were comprehensively evaluated. To guarantee robustness and reproducibility, a presence and variability filter was applied: only metabolites detected in 100% of the samples within a given group and exhibiting a coefficient of variation (CV) below 20% in quality control samples for LC-MS data (and below 30% for GC-MS data) were retained for subsequent analyses.

Multivariate statistical analysis (MVA) was performed using the open-access platform MetaboAnalyst 5.0, applying both



unsupervised and supervised methods such as principal component analysis (PCA) and orthogonal partial least squares discriminant analysis (OPLS-DA), with UV (unit variance) scaling. From the OPLS-DA model, variable importance in projection (VIP) scores were obtained to identify the metabolites contributing most to group separation, and 95% confidence intervals were estimated using the jackknife (JK) resampling method. To evaluate the statistical significance of individual metabolites, univariate analysis (UVA) was also carried out in MetaboAnalyst 5.0, including fold-change analysis and t-tests with false discovery rate (FDR) correction. Student's t tests were used to compare groups, and the resulting *p*-values were adjusted for multiple testing using Benjamini-Hochberg false discovery rate (FDR) correction. Metabolites were considered statistically significant if they met at least one of the following criteria: (1) a statistically significant *p* value (adjusted or unadjusted) and/or (2) a VIP score greater than 1 from the OPLS-DA model.

**2.6.5 Metabolite annotation and identification.** For features detected by liquid chromatography, multiple parameters were used to support metabolite annotation. These included verification of retention times, evaluation of possible adduct formation, and comparison of accurate high-resolution masses with publicly available databases using the CEU Mass Mediator tool (<http://ceumass.eps.uspceu.es>, accessed on May 2025). Theoretical molecular formulas were also generated based on isotopic distribution patterns. To further support compound identification, MS/MS fragmentation spectra were compared against reference spectra available in MS-DIAL (version 4.80), Lipid Annotator (version 10.0), and the Global Natural Products Social Molecular Networking (GNPS) platform. Additionally, the MS/MS spectra were manually interpreted to refine the identification of key features. For gas chromatography-based analysis, compound identification was achieved by comparing both the mass spectra and the retention indices (RIs) of the features against those reported in the Fiehn GC-MS Metabolomics RTL Library (2011 and 2013 versions).<sup>20</sup> Retention indices were determined using either FAMES (fatty acid methyl esters) or alkane standards ranging from C7 to C40. Finally, the confidence level for metabolite identification was assigned according to the criteria established by the Metabolomics Standards Initiative (MSI).<sup>18</sup>

**2.6.6 Preparation of quality control (QC) samples.** QC samples were prepared by pooling equal volumes of all individual extracts. To assess the reproducibility of sample preparation and the stability of the analytical platforms (LC-QTOF-MS and GC-QTOF-MS), several QC runs were performed to equilibrate the system. QC samples were subsequently randomly injected throughout the chromatographic sequence.

### 3. Results

Multivariate analysis reveals distinct metabolic profiles between nonextruded and extruded flours. The stability of the analytical platforms during sample acquisition was evaluated through PCA models (Fig. 1, Panels A-C). In these plots, the quality control (QC) samples (gray dots) clustered tightly, indicating

high analytical reproducibility across all platforms. Additionally, the PCA results revealed a clear separation trend between the nonextruded flour (NEF, blue dots) and extruded flour (EF, red dots) samples, suggesting that distinct metabolic fingerprints are associated with each processing condition.

This trend was further supported by the orthogonal partial least squares discriminant analysis (OPLS-DA) models (Fig. 1, Panels D-F), which revealed a pronounced separation between NEF and EF samples across all analytical platforms: LC-MS in positive (GM+), LC-MS in negative (GM-), and GC-MS modes. The OPLS-DA models showed strong explanatory and predictive capacity, with  $R^2$  values  $\geq 0.88$  and  $Q^2$  values  $\geq 0.84$ . Importantly, the high  $Q^2$  values in conjunction with statistically significant cross-validated ANOVA (CV-ANOVA,  $p < 0.05$ ) indicate robust model performance and suggest that the models are not overfitted.

Metabolomic analysis using both univariate and multivariate approaches resulted in the annotation of 124 differentially abundant metabolites between NEF and EF. Among these, 83% (103 metabolites) decreased after extrusion, whereas 17% (21 metabolites) increased in this group (Table S1). The annotated differentially abundant metabolites were distributed across various chemical classes. The most represented metabolites were fatty acyls (22 metabolites, 17.74%), followed by glycerophospholipids (18 metabolites, 14.52%) and organic acids (16 metabolites, 12.90%). Changes in the levels of amino acids and derivatives (14 metabolites, 11.29%) as well as those of carbohydrates and sugars (12 metabolites, 9.68%) were also detected. In lower proportions, differentially abundant flavonoids (8 metabolites, 6.45%), benzenoids (7 metabolites, 5.65%), and quinic acids and derivatives (6 metabolites, 4.84%) were identified. Finally, other classes, such as alkaloids, phenylpropanoids, organic nitrogen compounds, sphingolipids, terpenoids, purines, alcohols and polyols, and indoles and derivatives, accounted for less than 3% of the differentially abundant metabolites.

In terms of global trends, most chemical families exhibited a consistent reduction in their levels after the extrusion process. Here, the values in parentheses indicate the number of decreased metabolites relative to the total number of annotated metabolites in each class. This pattern was particularly evident for carbohydrates and sugars (12/12), glycerophospholipids (18/18), organic acids (12/16), quinic acids and derivatives (6/6), flavonoids (7/8), fatty acids (18/22), sphingolipids and derivatives (3/3), and terpenoids (4/4), which were predominantly decreased in the extruded flours. In contrast, other chemical classes, such as amino acids and derivatives (8/14) and alkaloids (1/3), did not show a homogeneous trend, with both increases and decreases observed among the metabolites in these groups.

Global trends are represented in Fig. 2, which presents the results of a detailed analysis of the 75 metabolites with the greatest variation between NEF and EF. In this heatmap, green-yellow represents metabolites with increased levels, whereas blue-violet tones indicate decreased levels. A clear separation is observed between the two experimental groups, with metabolites clustering into two main regions. The upper cluster corresponds to metabolites increased in nonextruded flours



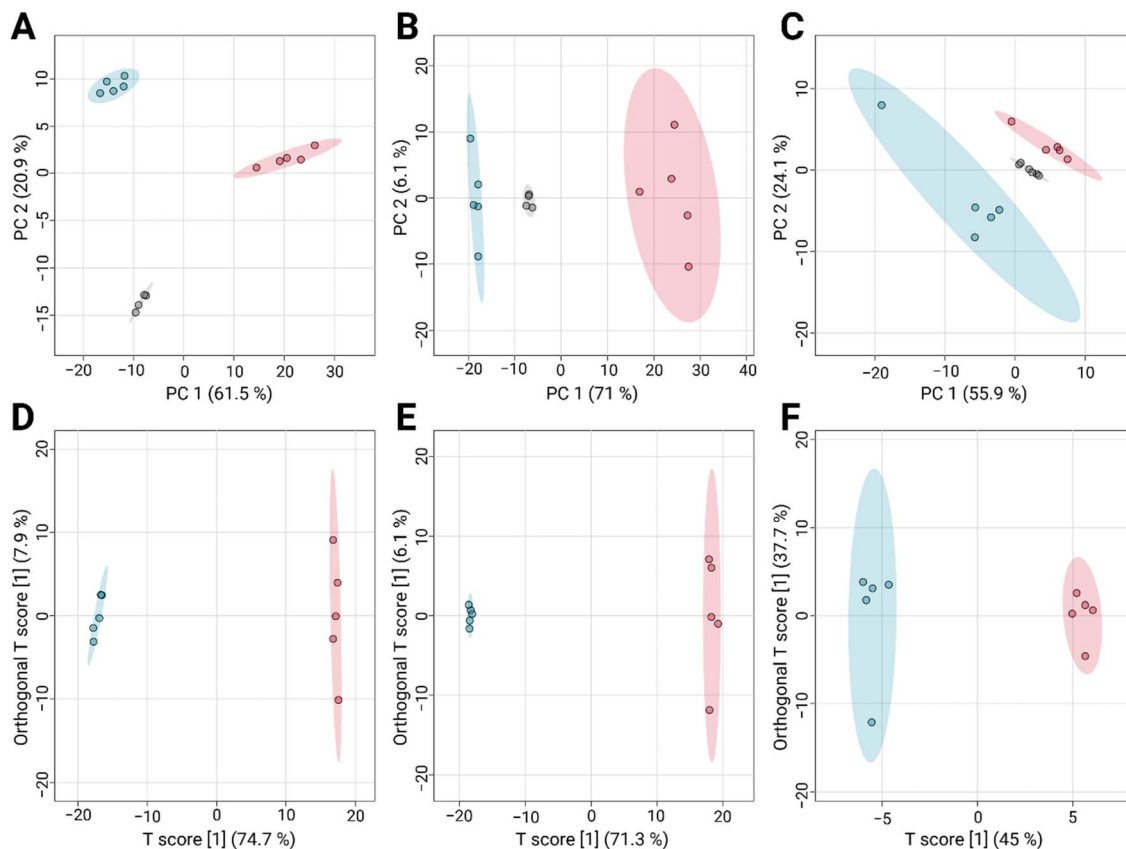


Fig. 1 Multivariate analysis of NEF and EF samples. (A–C) Principal component analysis; (D–F) orthogonal partial least squares discriminant analysis. Panels A and D correspond to LC–MS analysis in positive ionization mode; Panels B and E correspond to negative mode; and Panels C and F correspond to GC–MS analysis. (A)  $R^2$ : 0.96. (B)  $R^2$ : 0.88. (C)  $R^2$ : 0. (D)  $R^2$ : 0.97,  $Q^2$ : 0.95, CV-ANOVA:  $p < 0.05$  (E)  $R^2$ : 0.98,  $Q^2$ : 0.97, CV-ANOVA:  $p < 0.05$ . (F)  $R^2$ : 0.88,  $Q^2$ : 0.84, CV-ANOVA:  $p < 0.05$ . Samples from NEF are shown in blue, EF in red, and quality control (QC) samples in gray.

and is characterized by a heterogeneous composition, including sugars and glycerophospholipids, as well as some flavonoids, fatty acids, and terpenoids. In contrast, the lower cluster comprises metabolites decreased in nonextruded flours, mainly consisting of amino acids (*e.g.*, homoproline methyl ester and glycine), alkaloids (trigonelline and methylxanthine), and organic acids (gulonic acid and methoxycinnamaldehyde), among others.

The variations in protein, lipid, phenolic, and antioxidant parameters resulting from extrusion are summarized in Table 1. Protein and lipid contents decrease, whereas protein digestibility, total phenolic content and antioxidant activity showed a marked increase.

Collectively, these findings demonstrate that extrusion induces substantial modifications in the metabolic profiles of flours, primarily reflected in widespread decreases across several chemical families. These alterations indicate that extrusion influences not only structural components such as lipids and carbohydrates but also secondary metabolites associated with nutritional and functional properties, emphasizing the significant impact of this processing method on the chemical composition of flours.

## 4. Discussion

Composite flour was subjected to extrusion to evaluate the effects of thermomechanical processing on protein content and peptide composition. The protein content decreased significantly after extrusion ( $p < 0.05$ ), with an estimated reduction of 8.8%. Similar decreases have been reported for rye<sup>21</sup> and wheat flour.<sup>22</sup> The higher energy input and elevated temperatures during extrusion promote protein denaturation and aggregation, leading to intermolecular disulfide bond formation, enhanced cross-linking, and conformational changes.

Interestingly, although extrusion reduced crude protein content, a significant improvement in bioavailability was observed ( $p < 0.05$ ). Protein digestibility increased by approximately 42.9%, indicating that thermomechanical treatment promoted structural changes that enhanced protein accessibility to enzymatic hydrolysis. These changes may involve alterations in secondary protein structure,<sup>23,24</sup> exposure of hydrolysis sites, and inactivation of antinutritional compounds.<sup>24</sup> Previous studies have demonstrated that extrusion can inactivate or reduce the antinutritional effects of protein inhibitors and lectins in beans, thereby improving protein digestibility.<sup>25</sup> Similar improvements in digestibility





Fig. 2 Hierarchical clustering heatmap illustrating differences in metabolite abundance between nonextruded (NEF) and extruded (EF) flours. The abundance of each metabolite is represented according to the color scale, where yellow–green tones indicate increased metabolites, while blue–violet tones correspond to decreased metabolites. Samples from NEF are shown in blue, and those from EF are shown in red.

Table 1 Effect of extrusion on composition and antioxidant properties of composite flour from coffee and plantain byproducts<sup>a</sup>

Parameter	NEF	EF	Trend
Protein (%)	12.50 ± 0.12	11.40 ± 0.25	Decrease
Digestibility (%)	50.82 ± 3.44	72.62 ± 5.87	Increase
Lipids (%)	1.80 ± 0.06	0.08 ± 0.01	Decrease
TPC (mg GAE g <sup>-1</sup> dm)	5.38 ± 0.60	7.92 ± 1.00	Increase
DPPH (%)	24.57 ± 0.03	28.36 ± 0.02	Increase
ABTS (%)	59.49 ± 0.03	62.36 ± 0.04	Increase
TEAC (mM TE g <sup>-1</sup> dm <sup>-1</sup> )	2.392 ± 0.146	2.537 ± 0.176	Increase

<sup>a</sup> Values are expressed as mean ± standard deviation ( $n = 5$ ). NEF: non-extruded flour; EF: extruded flour.

have been reported for extruded soybean protein.<sup>23</sup> These findings highlight that the nutritional quality of proteins is determined by their concentration and bioavailability.

Extrusion, therefore, can enhance protein nutritional quality by improving its effective utilization.

Despite the improvement in protein digestibility, extrusion also induced qualitative changes in the amino acid profile. The levels of some essential amino acids, such as isoleucine (Ile) and tryptophan (Trp), decreased during extrusion, possibly because of thermal degradation or participation in Maillard reactions, especially in the presence of reducing sugars from plantain. According to Opazo-Navarrete *et al.*,<sup>24</sup> the development of a brown color during extrusion is linked to the depletion of essential amino acids such as lysine, resulting from their interactions with simple sugars. Similarly, non-essential amino acids (glutamine, Gln, and glutamic acid, Glu) decreased after extrusion.

The reduction in Glu can be associated with the production of pyroglutamic acid (PGA), which is formed by dehydration during the thermal processing of Glu.<sup>26</sup> This association is consistent with the observed increase in the PGA. This compound has industrial and biomedical relevance, with reported applications in pharmaceuticals, cosmetics, and agriculture. It also shows therapeutic potential for idiopathic pulmonary fibrosis<sup>27</sup> and antifungal activity.<sup>28</sup> On the other hand, the levels of asparagine (Asn) and glycine (Gly) increased after extrusion, possibly because of protein hydrolysis and structural changes associated with the redistribution of molecular weight, which involves a reduction in high-molecular-weight fractions and the formation of intermediate-weight protein aggregates.<sup>29</sup>

Similar changes in the amino acid profile have also been reported in extruded plant-based products, where sulfur-containing amino acids exhibit the greatest losses and tyrosine decreases in some formulations. These reductions have been attributed to oxidation reactions and Maillard-type pathways intensified under high-temperature, low-moisture conditions, as well as to the marked sensitivity of lysine to react with sugars. In contrast, methionine and cysteine are predominantly affected by oxidative processes that generate non-bioavailable derivatives.<sup>30</sup>

With respect to amino acid-derived compounds, a reduction was observed in amino sugars such as galactosamine, glucosamine-phosphate and glucosaminic acid, possibly as a result of degradation under extrusion temperatures. The melting points for these compounds are 182, 127 and 235 °C,<sup>31</sup> respectively, and extrusion was conducted at 160 °C in the central zone of the extruder. Conversely, ethanolamine and tyramine levels increased. Ethanolamine is recognized as a product of phosphatidylethanolamine degradation under exposure to high temperatures,<sup>32</sup> a phenomenon previously observed in coffee beans.<sup>32,33</sup> Tyramine can be formed by the decarboxylation of tyrosine, which is promoted by high temperatures.<sup>34</sup> Comparable degradation and decarboxylation pathways have been reported in other extruded matrices, where the combined effects of temperature and shear promote the formation of biogenic amines and amino alcohols, aligning with the observed increases in tyramine and ethanolamine during extrusion.<sup>30</sup>



With respect to lipids, the overall lipid content decreased markedly in EF; this reduction has been attributed to complex formation between monoglycerides, free fatty acids, amylose, and proteins.<sup>35</sup> Among the identified lipids, 18 corresponded to free fatty acids. Lipids are highly susceptible to oxidation during or after extrusion and are influenced by heat, light, and oxygen exposure<sup>36</sup> and pressure.<sup>37</sup> The mechanism for lipid oxidation has been previously explained.<sup>36</sup> Among the 43 lipid-derived compounds significantly affected by extrusion, 91% (39 compounds) decreased, whereas 9% (4 compounds) increased (Table S1). This reduction is consistent with the reduction in the overall lipid content and can be attributed to oxidative degradation, interactions with other compounds or oxidation, as mentioned above. Additionally, extrusion can induce the transformation of lipids, such as *via* isomerization, and the formation of new compounds. These changes can explain the increase in certain lipids, such as linolenic acid isomer 2, linoelaidic acid, *N*-myristylethanolamide, and stearamide.

The observed increase in the conjugated form of linolenic acid indicates that extrusion promotes changes in this fatty acid. A comparable trend was reported for white quinoa, where linoleic acid levels increased during extrusion.<sup>38</sup> Similarly, linoelaidic acid increased after extrusion. The generation of this trans isomer from linoleic acid has been reported to result from heat-induced isomerization.<sup>39</sup> This trans fatty acid is related to coronary disease and diabetes.<sup>40</sup> To the best of our knowledge, no studies have reported positive changes in *N*-myristylethanolamide or stearamide as a consequence of extrusion processing.

In cereal base (rice/corn), reductions in extractable fat have been attributed to the formation of amylose–lipid complexes (ALC), in which fatty acid chains become embedded within the amylose helix, thereby limiting their recoverability. This mechanism is more pronounced in matrices with higher amylose content, such as corn-based extrudates, and is further reinforced by the stronger hydrophobic interactions generated during extrusion between denatured proteins, starch, and lipids.<sup>41</sup> In addition, wholegrain extruded flours consistently exhibit substantial losses of polyunsaturated fatty acids, reflecting the combined effects of oxidative degradation and ALC formation. Processing conditions modulate the interplay between oxidation, isomerization, and complexation.<sup>42</sup>

Overall, carbohydrate and sugar levels decreased following extrusion. This reduction can be attributed to the processing conditions and food matrix composition, which favor starch gelatinization and Maillard reactions. During nonenzymatic browning, low-molecular-weight reducing sugars such as glucose, sorbose, galactose, mannose, 2-deoxy-ribose, and deoxyglucose react with free amino acids at high temperatures and relatively low moisture levels, resulting in the formation of a wide range of Maillard-derived compounds.<sup>43</sup> Similar results have been reported in twin-screw extrusion studies, where the reduction in reducing sugars and total sugars has been attributed to the Maillard reaction, as the compounds formed correlate with the increase in  $a^*$  values on the CIELab color scale.<sup>22</sup>

The decrease in nonreducing sugars can be explained by different degradation mechanisms. Compounds such as methyl-galactopyranoside, which contain a methylated O-glycosidic anomeric carbon, are susceptible to glycosidic bond hydrolysis under high-temperature, shear, and moisture conditions.<sup>44,45</sup> Additionally, lignin–carbohydrate interactions may promote the cleavage of glycosidic rings and the formation of furan derivatives, reducing anhydrosugars such as 1,5-anhydrosorbitol and sedoheptulose monohydrate anhydride.<sup>46</sup> In the case of sugar acids—including galacturonic, glucoheptonic, and mucic acids—their decline is associated with thermal degradation and decarboxylation reactions, where ring opening and CO<sub>2</sub> release result in smaller and more chromophoric molecules. These mechanisms, described for uronic acids,<sup>47</sup> also apply to aldonic and aldaric acids under high-temperature, high-shear conditions.

Consistent with these transformations, extrusion performed in brown rice flour have shown that starch gelatinization, granule disruption, and subsequent structural rearrangements, including the formation of amylose–lipid complexes, modify starch digestibility by accelerating early hydrolysis while promoting the generation of resistant starch fractions.<sup>48</sup>

Among organic acids, 16 compounds were identified, of which 12 decreased after extrusion. This trend reflects their susceptibility to thermal degradation under combined temperature, shear, and pressure effects. Extrusion may promote the decomposition of heat-labile phenolic acids or their interaction with nutrients released from the food matrix, resulting in reduced levels of compounds such as gallic and shikimic acids.<sup>49</sup> In addition, the thermal sensitivity of these acids is associated with their involvement in nonenzymatic browning reactions. Specifically, the thermal degradation of D-galacturonic acid, a uronic acid structurally related to glucuronolactone, results in rapid browning and the formation of carbocyclic and furan derivatives, which may also explain the observed increase in 2-furoic acid after extrusion.<sup>50</sup> Similarly, thermal treatment promotes decarboxylation and dehydration reactions in organic acids such as malic and citric acids, which participate in acrylamide formation pathways *via* the acrolein route.<sup>51</sup>

In this study, the total phenolic content (TPC) significantly increased ( $p < 0.05$ ), representing a 1.36-fold increase. This trend is consistent with previous reports in flaxseed meal, where extrusion increased the TPC and flavonoid fractions.<sup>52</sup> The observed increase can be explained by the breakdown of cell walls and protein–starch networks during thermomechanical processing, facilitating the release of bound phenolics into free fractions.<sup>53</sup> In our case, the remarkable increase in quercetin (6.73-fold) supports this mechanism through the hydrolysis of glycosides, resulting in the release of more bioavailable aglycones.

Nevertheless, previous studies have reported decreases in TPC after extrusion, indicating that the response is affected by the raw material and processing parameters.<sup>29</sup> In this work, extrusion caused a decrease in the levels of some specific phenolic compounds, such as procyanidins, catechins, rutin and hydroxycinnamic acid derivatives (chlorogenic,



caffeoylquinic, feruloylquinic, and dicaffeoylquinic acids), with fold changes ranging from 0.11 to 0.76 (Table S1). The observed reduction may be attributed to thermal degradation,<sup>29</sup> since most phenolic compounds are heat sensitive. Elevated temperatures can induce structural modifications that lead to the loss of functional properties.<sup>54</sup> This decrease is in agreement with the results of previous studies reporting the thermal degradation and oxidative decomposition of thermolabile phenolics during extrusion. Consistent with the TPC increase, the antioxidant activity also improved significantly after extrusion.

Among organic nitrogen compounds, caffeine decreased notably, standing out as one of the main metabolites derived from coffee pulp in the extruded mixture. Caffeine, a methylxanthine considered an antinutritional factor because of its negative impact on acceptability and palatability,<sup>55,56</sup> decreased significantly, which represents a positive outcome for extruded flour. Its reduction may be attributed to thermal degradation under high-temperature conditions.<sup>57</sup> In contrast, the levels of 2,5-dihydroxybenzaldehyde, 3-methylxanthine, and trigonelline increased by 2.52-, 1.58-, and 1.26-fold, respectively, after extrusion. These increases may result from high-pressure thermal treatment, which can promote the formation of trigonelline and phenolic compounds such as 2,5-dihydroxybenzaldehyde, as observed in studies on coffee beans processed under similar conditions.<sup>58</sup> The increase in 3-methylxanthine may be due to the degradation of caffeine, as this compound is a metabolite derived from 1,3,7-trimethylxanthine (caffeine).

In summary, extrusion as a thermal treatment reduces antinutritional compounds such as caffeine, but it can also cause partial degradation of bioactive compounds with antioxidant activity, such as phenols and flavonoids, as shown in Table S1. According to other authors, heat treatments effectively reduce antinutritional compounds such as tannins (*e.g.*, chlorogenic acid) and phytic acid.<sup>59</sup>

Among benzenoid compounds, benzoic acid, 3-methylbenzoic acid, and adenosine increased (Table S1). These changes may be related to the degradation of chlorogenic acid during thermal processing. It has been reported that heat treatment promotes the breakdown of chlorogenic acid, leading to the formation of aromatic phenolic derivatives and bitter compounds.<sup>57</sup> Both benzoic acid and 3-methylbenzoic acid are aromatic compounds, while adenosine contains adenine, which is an aromatic nitrogenous base.

Finally, extrusion technology represents an effective thermal pretreatment for the valorization of agro-industrial byproducts such as coffee pulp, plantain rachis, and rejected plantain. This process enables the production of precooked flour with a distinctive metabolomic profile, as demonstrated in this study, enhancing its functional and nutritional properties for human and animal nutrition. These findings open opportunities for developing high-value-added food products that support circular economics principles and reduce organic waste. Future studies should aim to optimize extrusion parameters and extend this approach to other agro-industrial residues.

## 5. Conclusions

Extrusion proved to be an effective strategy for transforming coffee and plantain byproducts into functional flours with enhanced nutritional and functional properties. These results demonstrate its potential for valorizing underutilized agro-industrial residues and its relevance as a processing technology for producing precooked flours that can be integrated into sustainable food systems. This approach aligns with the increasing demand for innovative ingredients that combine nutritional benefits with environmental responsibility.

At the metabolomic level, extrusion influenced both primary and secondary metabolites. Most compounds decreased, particularly carbohydrates, glycerophospholipids, and organic acids, while quercetin, total phenolic content, antioxidant activity, and protein digestibility increased. These results highlight the complex biochemical transformations triggered by thermomechanical processing and emphasize the need to optimize operating conditions to maximize nutritional advantages and ensure the suitability of agro-industrial byproducts as sustainable food ingredients.

These results demonstrate the role of extrusion as a transformative technology. The applied conditions enhanced the functional properties of the flour; however, the heterogeneous metabolite response highlights the need for careful optimization of the operational parameters. Future studies should focus on refining extrusion conditions to preserve key compounds, promote the release of bioactive metabolites, and reduce antinutritional substances. Furthermore, assessing the incorporation of these precooked flours into food formulations is essential for determining their nutritional, technological, and sensory performance.

## Author contributions

Laura Sofía Torres-Valenzuela and Jose Luis Plaza Dorado: conceptualization, supervision, project administration, formal analysis, methodology, writing – review & editing. Carolina Franco Urbano and Diana Paola Navia Porras: investigation, data curation, formal analysis, methodology, writing – review & editing. Monica Cala: methodology, resources, supervision, formal analysis, writing – review & editing.

## Conflicts of interest

There are no conflicts to declare.

## Data availability

All data supporting the findings of this study are included in the article.

Supplementary information (SI): Table S1. Details of the metabolites significantly affected in coffee and plantain by-product flours using gas chromatography–time-of-flight mass and liquid chromatography–time-of-flight mass. See DOI: <https://doi.org/10.1039/d5fb00698h>.



## Acknowledgements

The authors greatly appreciate the financial support from the National Financing Fund for Science, Technology and Innovation Francisco Jose de Caldas (Colombia), with the Orchids Program: Women in Science, Agents for Peace, Call 935-2023.

## Notes and references

- R. Khan, F. Anwar, F. M. Ghazali and N. A. Mahyudin, *Innovative Food Sci. Emerging Technol.*, 2024, **97**, 103828.
- W. Li, S. M. Pires, Z. Liu, X. Ma, J. Liang, Y. Jiang, J. Chen, J. Liang, S. Wang, L. Wang, Y. Wang, C. Meng, X. Huo, Z. Lan, S. Lai, C. Liu, H. Han, J. Liu, P. Fu and Y. Guo, *Food Control*, 2020, **118**, 107359.
- T. B. de Brito Nogueira, T. P. M. da Silva, D. de Araújo Luiz, C. J. de Andrade, L. M. de Andrade, M. S. L. Ferreira and A. E. C. Fai, *Environ. Sci. Pollut. Res.*, 2020, **27**, 18530–18540.
- L. A. Muñoz-Rios, J. Vargas-Villegas and A. Suarez, *Land Use Policy*, 2020, **91**, 104361.
- J. A. Gil-Gómez, L. M. Florez-Pardo and Y. C. Leguizamón-Vargas, *Discover Appl. Sci.*, 2024, **6**, 480.
- S. Hu, A. Gil-Ramírez, M. Martín-Trueba, V. Benítez, Y. Aguilera and M. A. Martín-Cabrejas, *Curr. Res. Food Sci.*, 2023, **6**, 100475.
- D. P. Navia-Porras, C. Franco-Urbano, L. S. Torres-Valenzuela, J. L. Plaza-Dorado and J. L. Hoyos-Concha, *Sustainability*, 2025, **17**(5), 1950.
- N. Yadav, D. Suvedi, A. Sharma, S. Khanal, R. Verma, D. Kumar, Z. Khan and L. Peter, *Food and Humanity*, 2025, **5**, 100672.
- L. Yafetto, G. T. Odamtten and M. Wiafe-Kwagyan, *Heliyon*, 2023, **9**, e14814.
- J. Delić, P. Ikonić, M. Jakanović, T. Peulić, B. Ikonić, V. Banjac, S. Vidosavljević, V. Stojkov and M. Hadnadev, *Innovative Food Sci. Emerging Technol.*, 2023, **87**, 103419.
- M. B. Gutierrez-Barrutia, S. Cozzano, P. Arcia and M. D. del Castillo, *Food Res. Int.*, 2023, **172**, 113160.
- A. Medic and C. Medana, *Appl. Sci.*, 2025, **15**, 8283.
- S. Md Nor, P. Ding, F. Abas and A. Mediani, *Agriculture*, 2022, **12**(2), 156.
- J. H. Suh, R. T. Madden, J. Sung, A. H. Chambers, J. Crane and Y. Wang, *J. Agric. Food Chem.*, 2022, **70**, 10389–10399.
- R. Apak, S. Gorinstein, V. Böhm, K. M. Schaich, M. Özyürek and K. Güçlü, *Pure Appl. Chem.*, 2013, **85**, 957–998.
- G. di G. Belinati, H. M. P. de Carvalho, E. L. de Almeida, A. R. de A. Nogueira and A. Virgilio, *Food Chem. Adv.*, 2025, **7**, 101016.
- D. C. Chigbo, S. I. Egba, I. S. E. Nwaorgu and B. C. Kenneth, *Food and Humanity*, 2025, **5**, 100680.
- Megazyme, *Protein digestibility assay procedure, Animal-Safe Accurate Protein Quality Score (ASAP-Quality Score Method) for determination of the Protein Digestibility Amino Acid Score*, 2019, [www.megazyme.com](http://www.megazyme.com), accessed 12/02/2025.
- W. Brand-Williams, M. E. Cuvelier and C. Berset, *LWT-Food Sci. Technol.*, 1995, **28**, 25–30.
- T. Kind, G. Wohlgemuth, D. Y. Lee, Y. Lu, M. Palazoglu, S. Shahbaz and O. Fiehn, *Anal. Chem.*, 2009, **81**, 10038–10048.
- A. Torbica, M. Belović, L. Popović and J. Čakarević, *Food Chem.*, 2021, **334**, 127523.
- Y. Wu, Z. Xiao, X. Jiang, C. Lv, J. Gao, J. Yuan, L. Shan and H. Chen, *J. Food Sci. Technol.*, 2022, **59**, 2655–2665.
- X. Fu, W. Li, T. Zhang, H. Li, M. Zang and X. Liu, *J. Sci. Food Agric.*, 2024, **104**, 2225–2232.
- M. Opazo-Navarrete, C. Burgos-Díaz, C. Bravo-Reyes, I. Gajardo-Poblete, M. Chacón-Fuentes, J. E. Reyes and L. Mojica, *Appl. Sci.*, 2025, **15**, 3538.
- L. C. Paula, A. C. Lemes, E. Valencia-Mejía, B. R. Moreira, T. S. Oliveira, I. T. N. Campos, H. F. S. Neri, C. Brondani, P. C. Ghedini, K. A. Batista and K. F. Fernandes, *Food Chem.:X*, 2022, **13**, 100259.
- Z. Zhu, Y. Bian, X. Zhang, R. Zeng and B. Yang, *Spectrochim. Acta, Part A*, 2022, **275**, 121150.
- Y. Wen, J. Nie, X. Qin and Z. Li, *J. Pharm. Biomed. Anal.*, 2025, 116967.
- L. Ai, S. Fu, Y. Li, M. Zuo, W. Huang, J. Huang, Z. Jin and Y. Chen, *Front. Plant Sci.*, 2022, **13**, 1102411.
- R. Y. Pismag, M. P. Polo, J. L. Hoyos, J. E. Bravo and D. F. Roa, *F1000Research*, 2024, **12**, 1356, DOI: [10.12688/f1000research.140748.2](https://doi.org/10.12688/f1000research.140748.2).
- P. Duque-Estrada, K. Hardiman, A. B. Dam, N. Dodge, M. D. Aaslyng and I. L. Petersen, *Food Funct.*, 2023, **14**, 7361–7374.
- Chem-Search Engine, ChemSrc, <https://www.chemsrc.com/en/>, accessed 20 May 2025.
- A. C. R. Silva, C. C. da Silva, R. Garrett and C. M. Rezende, *Food Res. Int.*, 2020, **137**, 109727.
- A. Zayed, A. Abdelwareth, T. A. Mohamed, H. A. Fahmy, A. Porzel, L. A. Wessjohann and M. A. Farag, *Food Chem.*, 2022, **373**, 131452.
- T. A. H. Nguyen, H. S. Rupasinghe, Q. H. Nguyen, T. N. M. Pham, Q. A. Hoang, B. Pham, T. K. Mai, T. H. H. Le, T. P. Q. Le and T. D. Mai, *J. Food Compos. Anal.*, 2025, **138**, 106997.
- E. H. Kamau, S. G. Nkhata and E. O. Ayua, *Food Sci. Nutr.*, 2020, **8**, 1753–1765.
- L. Hülsebusch, T. R. Heyn, J. Amft and K. Schwarz, *Food Chem.*, 2025, **470**, 142607.
- J. Zhang, P. E. Urriola, S. L. Naeve, G. C. Shurson and C. Chen, *Antioxidants*, 2023, **12**, 1419.
- J. Song and Y. Tang, *Food Res. Int.*, 2023, **169**, 112761.
- L. Wan, T. Li, M. Yao, B. Zhang, W. Zhang and J. Zhang, *Food Chem.:X*, 2024, **22**, 101328.
- Z. Xu, S. Liu, M. Shen, J. Xie and J. Yang, *Food Chem.*, 2022, **369**, 130930.
- D. Rico, A. B. Cano and A. B. Martín-Diana, *Molecules*, 2021, **26**, 5578.
- P. C. Torres-Aguilar, A. M. R. Hayes, X. Yepez, M. M. Martinez and B. R. Hamaker, *Int. J. Food Sci. Technol.*, 2023, **58**, 1336–1345.
- R. Y. Pismag, M. P. Polo, J. L. Hoyos, J. E. Bravo and D. F. Roa, *F1000Research*, 2024, **12**, 1356.



- 44 M. Brito-Arias, in *Synthesis and Characterization of Glycosides*, ed. M. Brito-Arias, Springer International Publishing, Cham, 2022, pp. 459–475.
- 45 X. Zhu, L. Yang, Z. Ge, W. Ouyang, J. Wang, M. Chen, Y. Yu, S. Wu, Y. Qin, C. Huang, G. Zhang, Y. Zhang, H. Yuan, Y. Jiang and J. Hua, *Curr. Res. Food Sci.*, 2025, **10**, 101037.
- 46 Y. Zhang, W. Xu, N. Ma, Y. Shen, F. Xu, Y. Wang, N. Wu, Z. Guo and L. Jiang, *Bioresour. Technol.*, 2022, **361**, 127714.
- 47 A. Fatouros, U. Einhorn-Stoll, H. Kastner, S. Drusch and L. W. Kroh, *J. Agric. Food Chem.*, 2021, **69**, 9376–9382.
- 48 G. Zhang, Y. Xuan, F. Lyu and Y. Ding, *Int. J. Biol. Macromol.*, 2023, **242**, 124594.
- 49 E. Šárka, M. Sluková and S. Henke, *Foods*, 2021, **10**, 2100.
- 50 M.-A. Bornik and L. W. Kroh, *J. Agric. Food Chem.*, 2013, **61**, 3494–3500.
- 51 D. N. Perera, G. G. Hewavitharana and S. B. Navaratne, *BioMed Res. Int.*, 2021, **2021**, 6258508.
- 52 L. Cheng, X. Liu, Y. Ma, X. Huang, X. Zhang, J. Liu, L. Song, M. Qiao, T. Li and T. Wang, *Food Chem.:X*, 2024, **24**, 101934.
- 53 J. Pico, K. Xu, M. Guo, Z. Mohamedshah, M. G. Ferruzzi and M. M. Martinez, *Food Chem.*, 2019, **297**, 124990.
- 54 Q. Wang, L. Li, T. Wang and X. Zheng, *Food Chem.*, 2022, **370**, 131361.
- 55 J. C. Osorio-Arias, Y. Duarte-Correa and L. S. Torres-Valenzuela, in *Coffee in Health and Disease Prevention*, ed. V. R. Preedy and V. B. Patel, Academic Press, 2nd edn, 2025, pp. 805–815.
- 56 G. Munguía-Ameca, M. E. Ortega-Cerrilla, J. G. Herrera-Haro, R. Bárcena-Gama, C. Nava-Cuéllar and P. Zetina-Córdoba, *Animals*, 2023, **13**(22), 3462.
- 57 K. Rzyska-Szczupak, A. Przybylska-Balcerek, M. Buško, L. Sz wajkowska-Michalek, T. Szablewski and K. Stuper-Szablewska, *Processes*, 2025, **13**(7), 2037.
- 58 W. Kim, S.-Y. Kim, D.-O. Kim, B.-Y. Kim and M.-Y. Baik, *Food Chem.*, 2018, **240**, 594–600.
- 59 C. M. Pontes, A. M. da Hora, L. P. Leal, L. da Fonseca Lima Herculano, M. I. C. Ferreira, I. L. Soares, K. M. Sá, M. N. de Oliveira and D. F. Pontes, *Food Chem.*, 2025, **493**, 146029.

